Journal of Inclusion Phenomena and Molecular Recognition in Chemistry **10**: 367–377, 1991.

A Possible Helical Model for Sodium Glycocholate Micellar Aggregates

ANNA RITA CAMPANELLI, SOFIA CANDELORO DE SANCTIS, LUCIANO GALANTINI and EDOARDO GIGLIO*
Dipartimento di Chimica, Università di Roma 'La Sapienza', P.le A. Moro 5, 00185 Roma, Italy.

LUCIO SCARAMUZZA
Istituto di Teoria e Struttura Elettronica e Comportamento Spettrochimico dei Composti di Coordinazione del C.N.R., Area della Ricerca, CP 10, 00016 Monterotondo Stazione, Roma, Italy.

(Received: 30 July 1990; in final form: 14 November 1990)

Abstract. Sodium glycocholate crystallizes in the tetragonal space group $I4$ with $a = b = 27.793(4)$, $c = 7.937(1)$ Å, and $Z = 8$. Refinement based on 2290 observed reflections led to a conventional $R = 0.10$. The bile salt molecules are arranged in a helix with 2_1 symmetry stabilized mainly by polar interactions. Four helices are held together by hydrogen bonds involving water molecules, giving rise to hydrophilic channels, with a small cross section, which can include water molecules. The packing of these tetramers form hydrophobic channels containing some disordered acetone and water molecules. The helices will be checked as a model for the micellar aggregates of this important conjugated bile salt, following the same strategy successfully applied to sodium deoxycholate.

Key words. Sodium glycocholate, X-ray crystal structure, micellar aggregate model.

Supplementary Data relating to this article are deposited with the British Library as Supplementary Publication No. SUP 82107 (20 pages).

1. Introduction

Bile salts, the most important natural detergents, form micellar aggregates in aqueous solutions and interact in bile and in the small intestines with several biological compounds as, for example, cholesterol, phospholipids, glycerides and fatty acids [1, 2]. Of course, knowledge of a bile salt micellar structure is crucial in order to understand its physicochemical and biological properties. Unfortunately, it is very difficult and often dangerous to infer structural models from the study of the liquid state, which generally provides results which are ambiguous in their interpretation. For this reason we have decided to resort to structural models, observed in the crystal state, in order to describe the structure of the micellar aggregates in aqueous solution, following the procedure satisfactorily employed, frequently, in macromolecular chemistry. Our strategy can be summarized as follows [3]:

(a) To find compounds that increase the size of their micellar aggregates by varying parameters such as ionic strength, pH or temperature, giving rise, subsequently, to all or some of the transitions: aqueous micellar solution → gel → macromolecular fibre → crystal.

*Author for correspondence.

(b) To verify that the X-ray diffraction patterns of the above mentioned phases show intensity maxima and minima in the same θ regions, in such a way as to have a good chance that the structural units present in all the phases are equal or very similar.
(c) To solve the structure of the crystal grown from an aqueous medium.
(d) To check the structural unit, observed in the crystal, as a model of the micellar aggregates in aqueous solution by means of small-angle X-ray scattering, extended X-ray absorption fine structure, nuclear magnetic resonance, electron spin resonance and circular dichroism techniques.

This procedure has been successfully applied to sodium and rubidium deoxycholate (NaDC and RbDC, respectively) [4–7]. Moreover, a similar study is in progress for sodium taurodeoxycholate (NaTDC) [8] and glycodeoxycholate (NaGDC) [9]. Again, helical models have been found, which now are under investigation using the techniques outlined under point *d*. Contemporaneously, the interaction between bile salt micellar aggregates and bilirubin-IXα [9], a spin-labeled cholestane which mimics cholesterol [10], acridine orange [11] and some hydrocarbons [5] have been analyzed in order to verify the helical models, to identify the micelle-probe binding sites and to obtain information on possible interaction mechanisms between bile salts and some important biological molecules.

The present paper deals with the beginning of a similar study (see point *c*) on sodium glycocholate (NaGC) which is the most abundant and one of the most important conjugated bile salts in man. Moreover, this work reports the first crystal structure of a conjugated derivative of cholic acid belonging to the pool of bile salts.

2. Experimental

2.1. CRYSTAL DATA

Single crystals of NaGC inclusion complexes with water and acetone were grown by diffusion of acetone vapour into an aqueous solution of the bile salt. After two or three days prismatic and colourless crystals, m.p. 473–475 K, were removed from the solution and used for the X-ray study.

Unit cell parameters were obtained by least squares from 25 centered reflections and refined together with the orientation matrix. The crystal data are as follows: $a = b = 27.793(4)$, $c = 7.937(1)$ Å , $V = 6131(1)$ Å^3, $Z = 8$, space group $I4$. The crystal density (1.27 g cm^{-3}) was obtained by flotation using both a chloroform-chlorobenzene and a chlorobenzene–bromobenzene mixture, the density of which was determined by means of a DMA 02C densimeter.

The inclusion of acetone in the crystals was checked by gas chromatography, using a Perkin-Elmer Sigma 1 model (FID detector) equipped with a 2 m × 2 mm i.d. column packed with Carbopack C (80/100 mesh) coated with 0.1% silicon SP 1000. A maximum weight percentage of 1.5% of acetone was detected when the crystals were in equilibrium with the acetone vapour.

A suitable single crystal of approximate dimensions 0.1 × 0.4 × 0.5 mm was sealed in a Lindemann glass capillary surrounded by mother liquor and mounted on a Nonius CAD4 diffractometer using graphite monochromated CuK_α radiation

($\lambda = 1.5418$ Å). A total of 2290 unique reflections with $I > 1.5\,\sigma(I)$ were recorded at room temperature by employing the ω-2θ scan mode in the range $6 \leqslant 2\theta \leqslant 140°$, the ω value being $(1.00 + 0.14 \tan\theta)°$. The scan speed changed from 1.6 to 5.5°/min as a function of the reflections intensity. Three standard reflections were monitored during collection, but negligible decay was observed. The data were corrected for Lorentz and polarization effects, but not for absorption ($\mu = 7.62\ \text{cm}^{-1}$).

2.2. STRUCTURE DETERMINATION AND REFINEMENT

The structure was solved by direct methods using the program MULTAN 88 [12] and refined by the full-matrix least-squares method with the program CRYSTALS [13]. Atomic scattering factors were taken from the *International Tables for X-ray Crystallography* [14]. Refinements of the non-H atoms were performed with anisotropic temperature factors while the hydrogens, generated at the expected positions, except the water and hydroxylic hydrogens which were not taken into account in any calculation, were refined with thermal parameters equal to the isotropic ones of the parent atoms. The atomic coordinates of the hydrogens were not refined. The function minimized was $\Sigma w(|F_o| - |F_c|)^2$ with $w = (\sin\theta/\lambda)^2$. Several other weighting schemes were checked, but the results were slightly worse.

Besides the NaGC atomic peaks five more peaks were observed and attributed to oxygens of water molecules, indicated as O_{W1}, O_{W2}, O_{W21}, O_{W3} and O_{W4}. An occupancy factor of 0.5 was assigned to O_{W2} and O_{W21}, about 1 Å apart, since their peaks showed nearly half the electron density of the other oxygen atoms. An occupancy factor of 0.25 was given to O_{W4} which lies on the 4-fold rotation axis. However, the calculated density, corresponding to the asymmetric unit NaGC + 3.25 H_2O, is 1.18 g cm^{-3}, much lower than the observed one (1.27 g cm^{-3}). On the other hand, inspection of the crystal packing (Figure 1) shows that there are empty channels, covered by nonpolar groups, around the 4_2 axes. These channels are large enough to easily accommodate a molecule such as acetone, found in the crystals by gas chromatography. Moreover, the presence of acetone within the channels is supported by the occurrence of large peaks, elongated along c. As a check an 'atomic' scattering factor g for acetone was introduced using the Debye formula [15]:

$$g^2 = \sum_{i=1}^{N} \sum_{j=1}^{N} f_i f_j \sin(4\pi r_{ij} \sin\theta/\lambda)/4\pi r_{ij} \sin\theta/\lambda$$

where N is the number of atoms, f_i and f_j the atomic scattering factors of atoms i and j, and r_{ij} the distance between atoms i and j. The computation of g was accomplished by the function

$$g = 20.0 \times \exp(-115.0s) + 6.5 \times \exp(-10.0s) + \\ + 2.5 \times \exp(-80.0s) + 3.0$$

where s is $(\sin\theta/\lambda)^2$. The inclusion of acetone in the refinement was crucial for fitting some strong low-angle reflections and gave rise to a significantly better agreement. At this stage two acetone molecules, linked by a water molecule forming hydrogen bonds with them, were introduced in the refinement with fixed atomic coordinates and isotropic thermal parameters and with an occupancy factor of

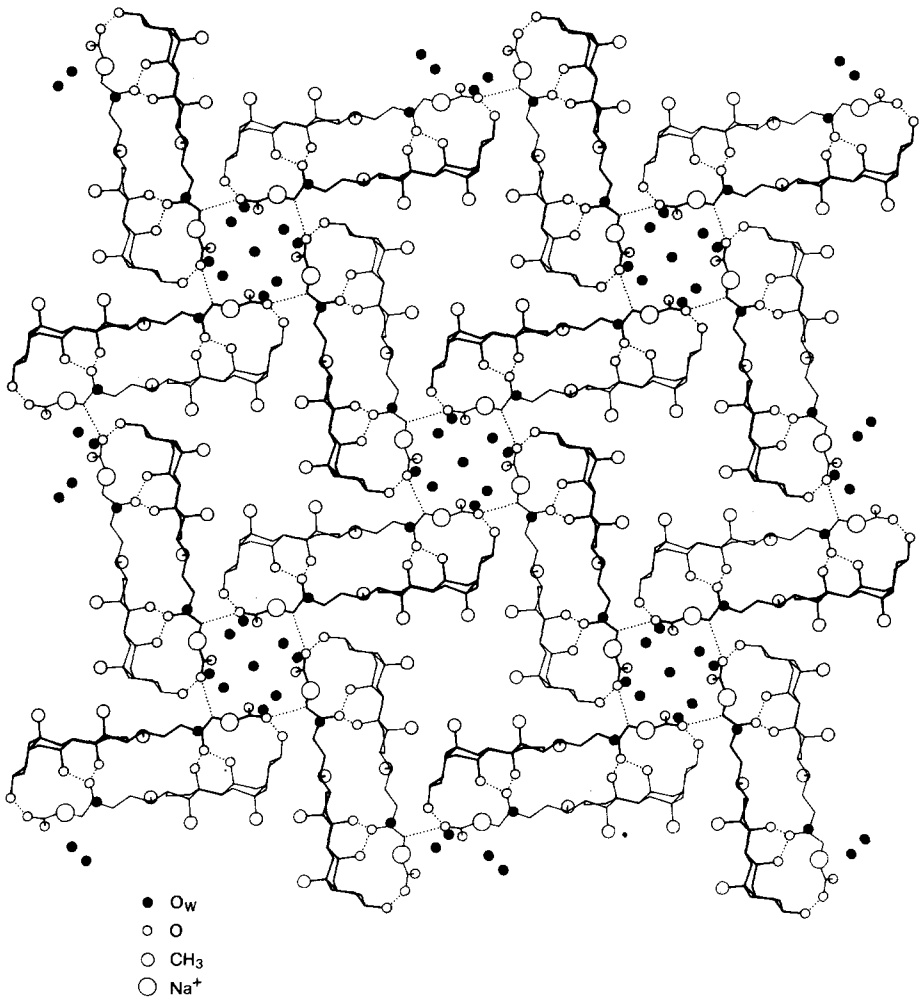

Fig. 1. NaGC crystal packing viewed along *c*. A thicker line represents an anion nearer to the observer. Dotted lines indicate some hydrogen bonds.

0.125. This system, identified by inspection of a Fourier synthesis, occupies two unit cells along *c* and accounts for some diffuse and weak intensity layers, observed in the oscillation photographs, which double the *c* axis.

The final agreement factors were $R = 0.10$ and $R_W = 0.11$. The atomic coordinates of O_{W1} and O_{W3} were kept fixed beginning from a late stage of the refinement since, otherwise, the corresponding distance became as short as 2.3 Å.

3. Results and Discussion

The atomic positional and thermal parameters are given in Table I, in accordance with the atom labelling of Figure 2, where bond distances and bond angles are

Table I. Fractional atomic coordinates ($\times 10^4$) and equivalent isotropic temperature factors ($\times 10^3$) together with the e.s.d's in parentheses

Atom	x/a	y/b	z/c	U_{eq}(Å^2)*
C(1)	5384(3)	2052(4)	5716(20)	65(4)
C(2)	5436(3)	2586(5)	5433(17)	66(4)
C(3)	5712(3)	2810(4)	6860(20)	66(3)
C(4)	5468(3)	2712(4)	8519(18)	58(3)
C(5)	5399(3)	2167(4)	8838(17)	57(3)
C(6)	5161(3)	2074(4)	10529(19)	63(3)
C(7)	4611(3)	2170(3)	10568(16)	49(3)
C(8)	4361(3)	1913(3)	9077(16)	44(2)
C(9)	4595(3)	2067(3)	7396(15)	40(2)
C(10)	5133(3)	1911(3)	7374(17)	50(3)
C(11)	4310(3)	1894(3)	5866(16)	48(3)
C(12)	3771(3)	1990(3)	5948(15)	44(3)
C(13)	3558(3)	1785(2)	7551[a]	38(2)
C(14)	3818(3)	2012(3)	9060(14)	36(2)
C(15)	3520(3)	1855(3)	10583(16)	47(3)
C(16)	3002(3)	1841(3)	9930(16)	46(3)
C(17)	3025(3)	1919(3)	7986(16)	41(2)
C(18)	3614(3)	1229(3)	7533(17)	47(3)
C(19)	5197(4)	1365(4)	7565(24)	78(4)
C(20)	2616(3)	1661(3)	7016(16)	42(2)
C(21)	2627(4)	1785(4)	5148(17)	61(3)
C(22)	2124(3)	1800(3)	7771(16)	49(3)
C(23)	1714(3)	1485(3)	7125(18)	52(3)
C(24)	1232(3)	1635(3)	7822(15)	43(3)
O(25)	5759(3)	3328(3)	6668(17)	85(3)
O(26)	4528(2)	2676(2)	10529(13)	54(2)
O(27)	3668(2)	2493(2)	5866(13)	51(2)
O(28)	1124(2)	2065(2)	7902(13)	55(2)
N(29)	945(2)	1293(3)	8407(16)	55(3)
C(30)	483(4)	1394(6)	9194(24)	85(5)
C(31)	46(4)	1215(4)	8281(22)	69(4)
O(32)	97(4)	1035(7)	6907(20)	141(7)
O(33)	−344(3)	1261(4)	8984(22)	121(6)
Na	4464(3)	3609(3)	9492(17)	147(4)
O_{W1}	4240[a]	4380[a]	10136[a]	206(9)
O_{W2}	1135(8)	1635(5)	2812(29)	77(7)
O_{W21}	1488(9)	1677(7)	2701(31)	90(7)
O_{W3}	1079[a]	102[a]	2980[a]	236(15)
O_{W4}	0[a]	0[a]	4843(96)	231(34)
C(1′)	5000	0	−568	250
C(2′)	4504	0	−1491	250
C(3′)	5496	0	−1491	250
O(1′)	5000	0	984	250
O_{W5}	5200	−250	4350	250
C(4′)	4900	0	8319	250
C(5′)	4611	−127	9981	250
C(6′)	5460	8	8219	250
O(2′)	4671	99	7026	250

*$U_{eq} = 1/3(\Sigma_i \Sigma_j U_{ij} \boldsymbol{a}_i \cdot \boldsymbol{a}_j a_i^* \cdot a_j^*)$, where U_{ij} are thermal parameters, expressed as mean-square amplitudes of vibration, and $\boldsymbol{a}$ and a^* are unit cell direct axis and reciprocal axis moduli, respectively.
[a]These coordinates were kept fixed during the refinement.

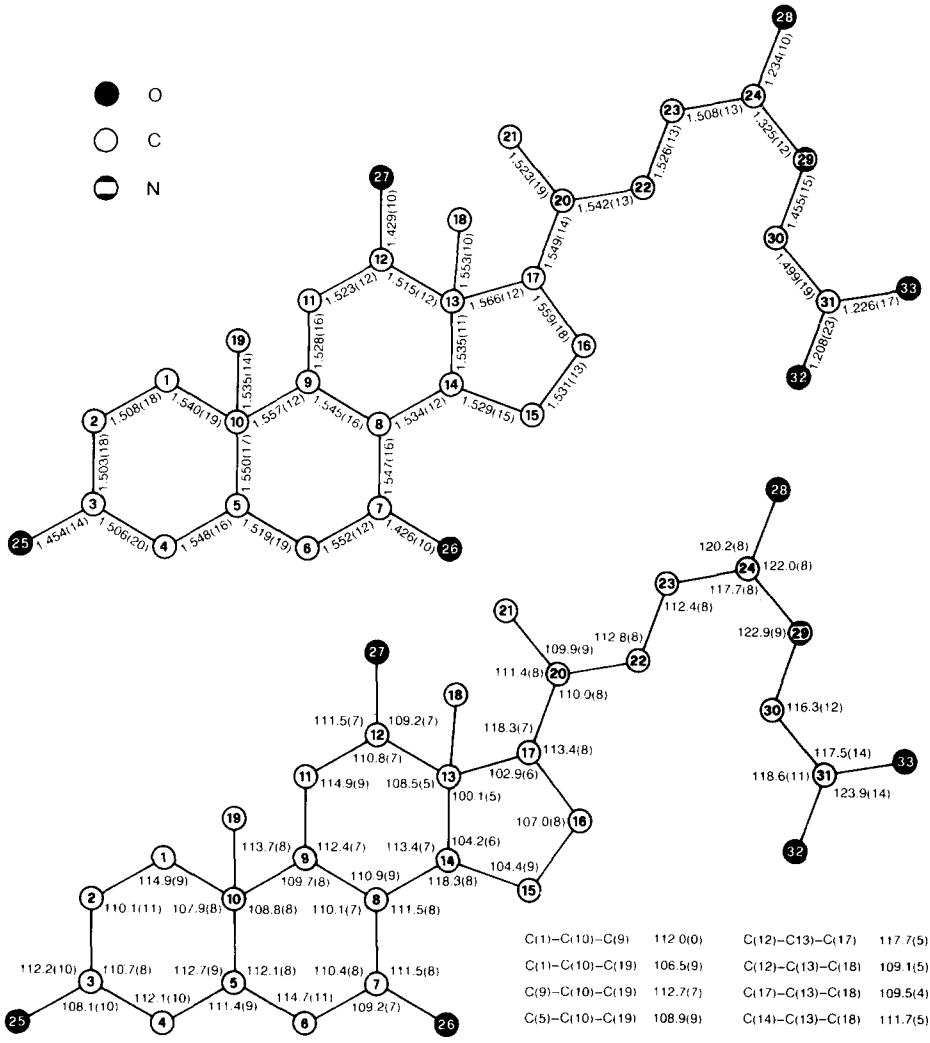

Fig. 2. Final geometry found for the glycocholate anion. Bond distances (Å) above and bond angles (°) below. The e.s.d's in parentheses.

reported. All the atoms labelled A belong to the acetone molecules forming hydrogen bonds with O_{W5}.

The structure factors list has been deposited as Supplementary Data.

3.1. MOLECULAR STRUCTURE

The slightly high R factor (0.10) reflects the difficulty in locating the acetone molecules that, very likely, can give rise to positional disorder. However, the satisfactory geometry of NaGC (see Figure 2) supports the correctness of the structure.

Table II. Torsion angles of the NaGC side chain and ring D together with Δ and φ_m(°). Estimated standard deviations in parentheses. The values of NaGDC together with some values from Ref. 18 are also given

	NaGC	NaGDC	NaTC	NaTC	Ref. 18
C(13)—C(17)—C(20)—C(21)	−64.5(11)	−39(4)	−50.7(8)	−59.9(8)	−49
C(13)—C(17)—C(20)—C(22)	173.5(8)	−166(2)	−176.3(5)	175.5(5)	−170
C(17)—C(20)—C(22)—C(23)	−168.3(8)	−173(2)	69.3(7)	69.3(7)	61
C(20)—C(22)—C(23)—C(24)	−177.9(8)	−166(2)	89.5(7)	−155.6(6)	180
C(22)—C(23)—C(24)—O(28)	43.1(13)	53(4)	50.8(9)	−70.7(9)	180
C(22)—C(23)—C(24)—N(29)	−133.8(10)	−123(3)	−130.1(6)	108.0(9)	0
C(23)—C(24)—N(29)—C(30)	176(11)	178(3)	−174.2(6)	160.9	180
C(24)—N(29)—C(30)—C(31)	114.8(14)	−158(3)	−79.6(7)	115.5	−66
O(28)—C(24)—N(29)—C(30)	−0.3(17)	2(5)	5.0(10)	−20.4	0
N(29)—C(30)—C(31)—O(32)	−5.8(21)	−20(4)			
N(29)—C(30)—C(31)—O(33)	174.2(13)	168(3)			
C(17)—C(13)—C(14)—C(15)	46.1(8)	44(2)	49.3(5)	48.2(5)	46
C(13)—C(14)—C(15)—C(16)	−34.0(9)	−32(3)	−38.7(6)	−36.8(6)	−33
C(14)—C(15)—C(16)—C(17)	7.9(10)	8(3)	13.1(6)	10.9(6)	8
C(15)—C(16)—C(17)—C(13)	20.2(9)	19(3)	17.1(6)	18.7(6)	20
C(16)—C(17)—C(13)—C(14)	−40.0(8)	−38(2)	−39.9(6)	−40.5(5)	−39
Δ	14.7	14	3.9	9.0	15
φ_m	46.5	44	49.3	48.3	46

Ring D adopts a conformation intermediate between the half-chair and the β envelope symmetry as in the case of RbDC [4], NaTDC [8], and NaGDC [9]. The corresponding torsion angles, calculated on the basis of the convention of Klyne and Prelog [16], are reported together with the phase angle of pseudorotation Δ and the maximum angle of torsion φ_m [17] in Table II.

The side chain conformation (see Table II) deserves some attention. It can be compared with that of NaGDC [9] and with that proposed in a submicellar aqueous solution of dysprosium glycocholate on the basis of a paramagnetic NMR study and potential energy calculations [18]. The comparison with NaGDC shows that the two side chain conformations are approximately extended and similar up to the amide group, the major difference being the C(13)—C(17)—C(20)—C(21) and, to a lesser extent, the C(13)—C(17)—C(20)—C(22) torsion angles, which present unusual values for NaGDC [9], probably owing to packing requirements. After the amide group, a very different torsion angle occurs about the N(29)—C(30) bond but, subsequently, there is a qualitative agreement between the arrangements of the carboxylic group. On the contrary, the conformation proposed in Ref. 18 does not match, at least in part, those of NaGC and NaGDC (see Table II). The main feature of this conformation is the *gauche* state of the torsion angle C(17)—C(20)—C(22)—C(23) (61°), which corresponds to a relative energy minimum [19] and is invariably found, for example, in the orthorhombic and tetragonal inclusion compounds of deoxycholic acid [20, 21 and references quoted therein] and in a crystal phase of RbDC grown from organic solvents [22]. In all these crystals the structural unit is a bilayer and, generally, the Δ value is within the range 0–12°,

with ring D approaching the half-chair symmetry. On the other hand, when the structural unit is a helix, as for hexagonal inclusion compounds of deoxycholic acid [23], a crystal phase of RbDC grown from water [4], NaGDC [9], NaTDC [8] and NaGC, the Δ value lies, generally, within the range 10–24°, with ring D approaching the β envelope symmetry [19]. The torsion angles of Ref. 18, although differing from those observed in the crystal structures, are, in principle, possible both because of their high conformational flexibility and their having been determined in a very dilute solution. It does however seem improbable that the two related torsion angles C(22)—C(23)—C(24)—O(28) and C(22)—C(23)—C(24)—N(29) are approximately 180° and 0°, respectively. In fact, the corresponding values of NaGC, NaGDC and NaTDC are within the range 43–65° and 226 – 248°. Moreover, we have solved the crystal structure of a triclinic phase of sodium taurocholate containing two molecules in the asymmetric unit (our unpublished results) both with the C(17)—C(20)—C(22)—C(23) angles in *gauche* conformations, as in Ref. 18, and also in these cases the torsion angles around the C(23)—C(24) bond are very far from 180° and 0° (51 and −130° in one molecule and −71 and 108° in the other molecule). It seems better to adopt for ring D in the conformational analysis of the NaGC side chain in Ref. 18 a Δ value smaller than 15°, since this value is generally coupled with a C(17)—C(20)—C(22)—C(23) torsion angle of about −170° [19] and not with a value of 61° (see Table II).

3.2. CRYSTAL PACKING

The structural unit observed in the crystal is the 2_1 helix projected in Figure 3 along *b*, perpendicularly to the helical axis parallel to *c*. The sodium ion, O_{W2} and O_{W3}, which contribute to the stability of the helix, are shown. The main ion–ion and ion-dipole interactions together with the hydrogen bonds formed by sodium ion and water molecules are shown in Figure 4. The hydrogen bonds formed by the hydroxyl and carboxyl groups of the NaGC anion involve O(25) with O(33) (2.68 Å) and O(28) with O(26) and O(27) (2.71 and 2.72 Å, respectively). The very short $O_{W1} \cdots O_{W3}$ distance seems to indicate that the two atoms, or at least one of them, are suffering from positional disorder.

The helix has an approximate ellipsoidal cross section, perpendicular to the helical axis, with semimajor and semiminor axes of about 19 and 8 Å, respectively, taking into account for the value of the semiminor axis the most protruding C(18) and C(19) methyl groups. The helical outer surface is polar around the end region of the semimajor axis and nonpolar elsewhere, thus displaying an increase in polarity with respect to NaGDC. Therefore, the same sequence in the polarity of the single molecule, NaGC > NaGDC > NaDC, is preserved in the corresponding helical models proposed for the micellar aggregates [9]. The helix can be permeable to the water molecules of the solvent owing to the sufficient separation between two anions, related by a *c* translation along the helical axis. This separation becomes larger in the side chain region, so that the helix could be easily filled by water molecules if it exists in aqueous medium.

An aggregation of helices may be hypothesized under proper conditions of concentration, ionic strength, temperature, etc. Inspection of the crystal packing shows the occurrence of tetramers, located around hydrophilic channels having a

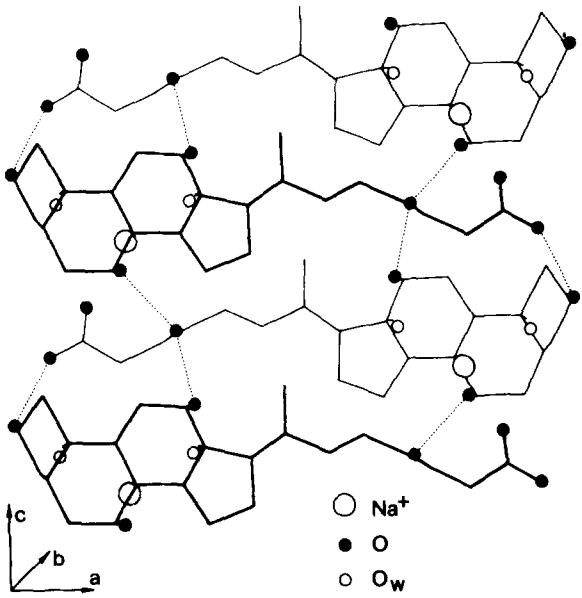

Fig. 3. View of the 2_1 helix projected along *b*. A thicker line represents an anion nearer to the observer. Only the hydrogen bonds formed by the oxygen atoms of NaGC anions are shown by broken lines.

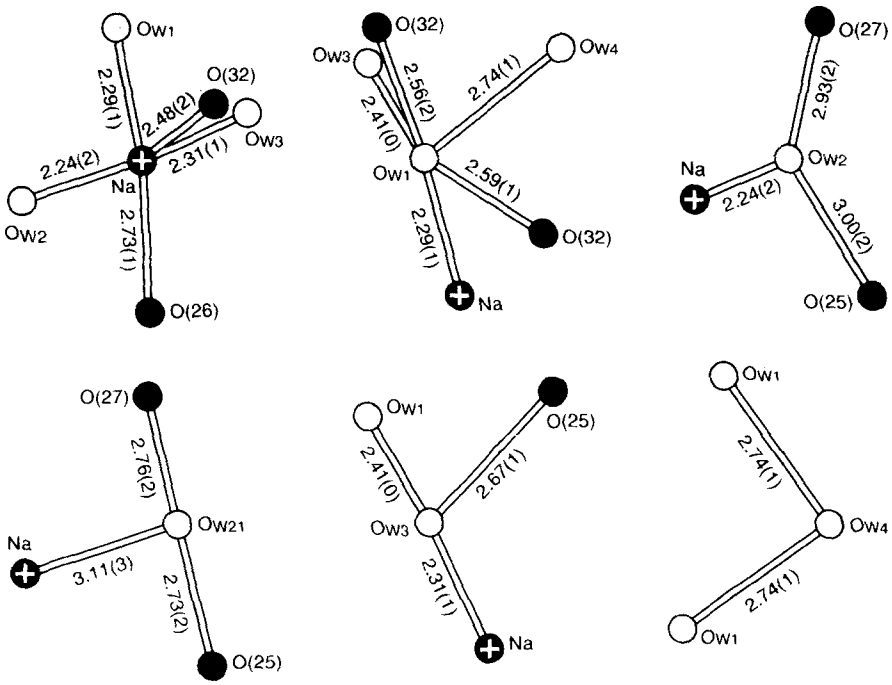

Fig. 4. Coordination of sodium ion and water molecules viewed along *c*. The distances (Å) are reported together with their e.s.d's in parentheses.

small cross section, centred on the four-fold rotation axes. The four helices of a tetramer are mainly held together by the hydrogen bonds and the ion-dipole interaction involving O_{W1} (see Figure 4), by the hydrogen bond between N—H and the O(33) of a carboxylic group (2.82 Å), and the hydrogen bond between O_{W2} (or O_{W21}) and O(25).

The packing of these tetramers gives rise to the formation of hydrophobic channels, centred on the 4_2 axes (Figure 1), in which the main interactions are of the van der Waals type. No strong intermolecular interactions occur among NaGC anions and, hence, the inclusion of acetone improves the packing stability, especially by means of contacts involving the C(19) methyl group of NaGC and those of acetone.

A last point deserves some attention. The density calculated assuming the asymmetric unit NaGC + 3.375 H_2O + 0.25 acetone is only 1.22 g cm^{-3}, much lower than the observed value of 1.27 g cm^{-3}, obtained by flotation using a chloroform–chlorobenzene or a chlorobenzene–bromobenzene mixture. This result questions the correctness of the crystal structure. However, the acetone molecules can easily escape from the crystal, so that it can be reasonably supposed that they can be replaced by the molecules of the liquid used for the density measurements, since the hydrophobic channels have enough room to accommodate chlorobenzene and bromobenzene molecules. The chlorine or bromine atoms can, therefore, be responsible for the measured high density value.

4. Concluding Remarks

The helical model of NaGC identified in the crystal structure is promising and will be checked in the study of aqueous micellar solutions. The observed helix is very different from that determined for NaDC and RbDC and from those proposed for NaGDC and NaTDC, now under investigation, and can be expected owing to the dissimilar physico-chemical properties of the bile salts. Even in the case of the very similar molecules NaGDC and NaGC there are basic properties such as the critical micellar concentration and the aggregation number that vary considerably [24] and that can be more reasonably accounted for by micellar aggregates with different structures rather than with a unique structure [25]. The water molecules of the solvent easily permeate into the binary helix, which is characterized by a greater polarity of the outer surface than NaDC and NaGDC, thus explaining the decrease of hydrophobicity in the order NaDC > NaGDC > NaGC, in accordance with measurements of equilibrium cholesterol-solubilizing capacity [26].

Lastly, the NaGC molecular geometry confirms the high conformational flexibility around some bonds of the side chain of the bile salt anions, caused by their ability to form polar interactions.

Acknowledgement

The authors wish to thank Professor M. Di Vaira (University of Florence) for data collection. The Italian Ministero dell'Università e della Ricerca Scientifica e Tecnologica and the Italian Consiglio Nazionale delle Ricerche – Progetto Finalizzato Chimica Fine e Secondaria – are gratefully acknowledged for financial support.

References

1. M. C. Carey and D. M. Small: *J. Clin Invest.* **61**, 998 (1978).
2. A. F. Hofmann: *Biochem. J.* **89**, 57 (1963).
3. A. R. Campanelli, S. Candeloro De Sanctis, E. Giglio, N. V. Pavel, and C. Quagliata: *J. Incl. Phenom.* **7**, 391 (1989).
4. A. R. Campanelli, S. Candeloro De Sanctis, E. Giglio, and S. Petriconi: *Acta Crystallogr.* Sect. **C40**, 631 (1984).
5. G. Conte, R. Di Blasi, E. Giglio, A. Parretta, and N. V. Pavel: *J. Phys. Chem.* **88**, 5720 (1984).
6. G. Esposito, E. Giglio, N. V. Pavel, and A. Zanobi: *J. Phys. Chem.* **91**, 356 (1987).
7. E. Giglio, S. Loreti, and N. V. Pavel: *J. Phys. Chem.* **92**, 2858 (1988).
8. A. R. Campanelli, S. Candeloro De Sanctis, E. Giglio, and L. Scaramuzza: *J. Lipid Res.* **28**, 483 (1987).
9. A. R. Campanelli, S. Candeloro De Sanctis, E. Chiessi, M. D'Alagni, E. Giglio, and L. Scaramuzza: *J. Phys. Chem.* **93**, 1536 (1989).
10. G. Esposito, A. Zanobi, E. Giglio, N. V. Pavel, and I. D. Campbell: *J. Phys. Chem.* **91**, 83 (1987).
11. E. Chiessi, M. D'Alagni, G. Esposito, and E. Giglio: paper submitted for publication to *J. Incl. Phenom.* (1990).
12. T. Debaerdemaeker, G. Germain, P. Main, L. S. Refaat, C. Tate, and M. M. Woolfson: *MULTAN 88.* Computer Programs for the Automatic Solution of Crystal Structures from X-ray Diffraction Data. University of York, England (1988).
13. D. J. Watkin, and J. R. Carruthers: *CRYSTALS User Guide*, Chemical Crystallography Laboratory, University of Oxford, England (1981).
14. *International Tables for X-Ray Crystallography*, Vol. 4, J. A. Ibers and W. C. Hamilton, Kynoch Press, Birmingham, England, 1974, p. 99. Distributed by Kluwer Academic Publishers.
15. P. Debye: *Ann. Phys. (Leipzig)* **46**, 809 (1915).
16. W. Klyne and V. Prelog: *Experientia* **16**, 521 (1960).
17. C. Altona, H. J. Geise, and C. Romers: *Tetrahedron* **24**, 13 (1968).
18. E. Mukidjam, G. A. Elgavish and S. Barnes: *Biochemistry* **26**, 6785 (1987).
19. E. Giglio and C. Quagliata: *Acta Crystallogr.* **B31**, 743 (1975).
20. E. Giglio In *Inclusion Compounds*, Vol. 2 (Eds. J. L. Atwood, J. E. D. Davies, and D. D. MacNicol), ch. 7, p. 207, Academic Press (1984).
21. E. Giglio, F. Mazza, and L. Scaramuzza: *J. Incl. Phenom.* **3**, 437 (1985).
22. V. M. Coiro, E. Giglio, S. Morosetti, and A. Palleschi: *Acta Crystallogr.* **B36**, 1478 (1980).
23. S. Candeloro De Sanctis, V. M. Coiro, E. Giglio, S. Pagliuca, N. V. Pavel, and C. Quagliata: *Acta Crystallogr.* **B34**, 1928 (1978).
24. C. A. Jones, A. F. Hofmann, K. J. Mysels, and A. Roda: *J. Colloid Interface Sci.* **114**, 452 (1986).
25. D. M. Small, S. A. Penkett, and D. Chapman: *Biochim. Biophys. Acta* **176**, 178 (1969).
26. M. J. Armstrong and M. C. Carey: *J. Lipid Res.* **23**, 70 (1982).